L.I. Nykyruy *Ph.D. Proffesor*[1], **O.M. Voznyak** *Ph.D. Proffesor*[1],
Y.S. Yavorskiy *Ph.D*[1], **V.A. Shenderovskiy** *Dr.Sci., Professor*[2],
R.O. Dzumedzey[1], **O.B. Kostyuk**[1], **R.I. Zapukhlyak** *Ph.D.*[1]

[1]Vasyl Stefanyk Precarpathian National University, 57, Shevchenko Str.,
Ivano-Frankivsk, 76018, Ukraine,
[2]Institute of Physics NAS of Ukraine, 46, Nauky Av., Kyiv, 02000, Ukraine

INFLUENCE OF THE BEHAVIOR OF CHARGE CARRIERS ON THE THERMOELECTRIC PROPERTIES OF *PbTe:Bi* THIN FILMS

The influence of technological factors of thin film deposition by the method of open evaporation in vacuum on the realization of charge carrier scattering processes is investigated. The contribution to the transport phenomena of carrier scattering for PbTe:Bi films deposited on the muscovite mica and glass ceramic (sitall) (0001) substrates are determined. In particular, the surface-bound carriers (Fuchs and Sondheimer theory) and grain boundaries (Meijdes and Shatskis theory) are analyzed. The choice of the type of substrate material and the temperature modes of the deposition changed the structure of the film surface and, accordingly, the values of thermoelectric parameters of the initial material. In particular, the selection of experimental modes allows manipulating the grain size and the thickness of the film. Glass ceramic (sitall) substrates contribute to a significantly smaller grain size compared with the use of mica substrates. It is shown that the effects of grain boundaries scattering are dominant for all films. The surface effects are only significant for sufficiently thin films the thickness of which is commensurate with the mean free path of charge carriers. Bibl. 46, Fig. 3, Table 3.
Key words: thermoelectricity, thin films, surface, grain boundaries, charge carrier scattering.

Introduction

The thermoelectric energy conversion annually increases the potential of its practical application. This is caused by a number of factors: the possibility of direct conversion of heat into electricity without the use of mobile mechanisms, positive environmental impact, reliability and accuracy in operation [1, 2]. Thus, the conversion of the heat of exhaust gases into electric energy at combustion of various types of fuels has a positive effect on the global reduction of the greenhouse effect [3 – 5]. Sometimes only thermoelectricity allows electricity generation when there are no other available sources, such as power lines.

The quality of final devices – thermoelectric modules, or individual thermoelements, is conventionally determined by the value of the dimensionless thermoelectric figure of merit ZT:

$$ZT = \frac{S^2\sigma}{\chi}T\,, \qquad (1)$$

where S is the Seebeck coefficient, σ is the electrical conductivity, χ is the coefficient of thermal conductivity, T is the absolute temperature, Z is the thermoelectric figure of merit of the thermoelectric material.

The value of *ZT* for most modern industrial thermoelements is 0.4 – 0.7 [6] or for the best within 1.0 [7]. For the studies of laboratory materials, this value is significantly higher: 1.1 for doped *SnTe* [8, 9] 1.6 – 1.8 for $PbTe_{1-x}Se_x$ [10], 1.7 for Mg_3Sb_2 [11] or 2.2 for $Pb_{18}Ag_2Te_{20}$ [12, 13].

Concerning final industrial devices – thermoelectric generators, their efficiency values are (4 – 6) % [6, 14]. These are sufficiently high values taking into account almost free of charge sources of heat for the generation of thermoelectric energy. These efficiency values provide a decent economic competition for thermoelectric generating devices to other alternative energy sources. On the other hand, thermoelectric devices are characterized by the reliability, durability in operation and have a positive effect on the improvement of environmental situation.

The thin-film thermoelectric devices deserve special attention [15 – 18]. They have a number of features. On the one hand, they generate several fold less energy than traditional macroscopic devices. But, on the other hand, the thin-film micro-generators of energy are indispensable for use in miniature devices, for example, for medicine or electronics. Also, one should note their significantly lower cost and higher technical characteristics. Thus, [19] shows the possibility of achieving $ZT \sim 2.5$ for $PbSe_{0.98}Te_{0.02} / PbTe$, *PbSnSeTe* / *PbTe* or Bi_2Te_3 / Sb_2Te_3 quantum dot heterostructures. The thin films arouse the interest of researchers due to their different peculiarities. On the one hand, it is the possibility of significant improvement of certain features, in particular, thermoelectric properties, due to diminishing their size [20 – 24]. On the other hand, an important role is played by the miniaturization of final devices. On the basis of thin films it is possible to create thermoelectric micro-modules that will have practical use in miniature devices, where conventional thermoelectric modules cannot be placed due to their dimensions [25 – 27].

This paper analyzes the possibility of using bismuth doped *PbTe* thin films for thermoelectric energy conversion. For this purpose, the study of the thermoelectric properties of *PbTe*:*Bi* thin films deposited on mica and sitall substrates was performed.

Experiment

The *PbTe:Bi* doped films were obtained by vapour phase deposition using open vacuum evaporation method. As materials, freshly cleaved muscovite mica and sitall (0001) substrates were chosen. For the films on mica substrates the following technological modes were used: the temperature of evaporator was $T_E = 970$ K, and the temperature of the substrates varied $T_S = (420 – 470)$ K. The thickness of thin films within (0.08 – 1.2) μm was sometimes set by the time of deposition (5 – 45) min and determined using microinterferometer MII-4 and the Dektak XT profilograph with application of the digital image processing methods. When the films were deposited on the sitall substrates, the temperature of the evaporator varied in the range of $T_E = (920 – 1020)$ K, the temperature of the substrates varied in range of $T_S = (420 – 520)$ K, and the deposition time was chosen from $\tau = 3$ sec to 120 sec. The presence of specially designed oven that included five heaters of substrates made it possible to obtain films of different thicknesses in one technological process.

Four Hall and two current contacts were applied on the measurement sample. Electrical parameters were measured in constant electric and magnetic fields. The magnetic field is directed perpendicular to the film surface at induction of 2 T. Silver films were used as ohmic contacts. The current through the sample was ~ 3 mA.

The structure of the films was investigated by Atomic Force Microscopy (AFM) methods using Nanoscope 3a Dimension 3000 (Digital Instruments USA). Measurements were made in the central part of the samples using serial silicon probes NSG-11. The AFM data were processed in the Gwyddion program (surface topology, nanocrystal size, etc.). The AFM images of the surface of obtained films are shown in Fig. 1, and the technological modes for these *PbTe:Bi* films are given in Table 1. The grain sizes on the

surface of the crystallites were determined by processing the images obtained on Nexus 412 A microscope using the specialized INNOVATEST Hardworx software package.

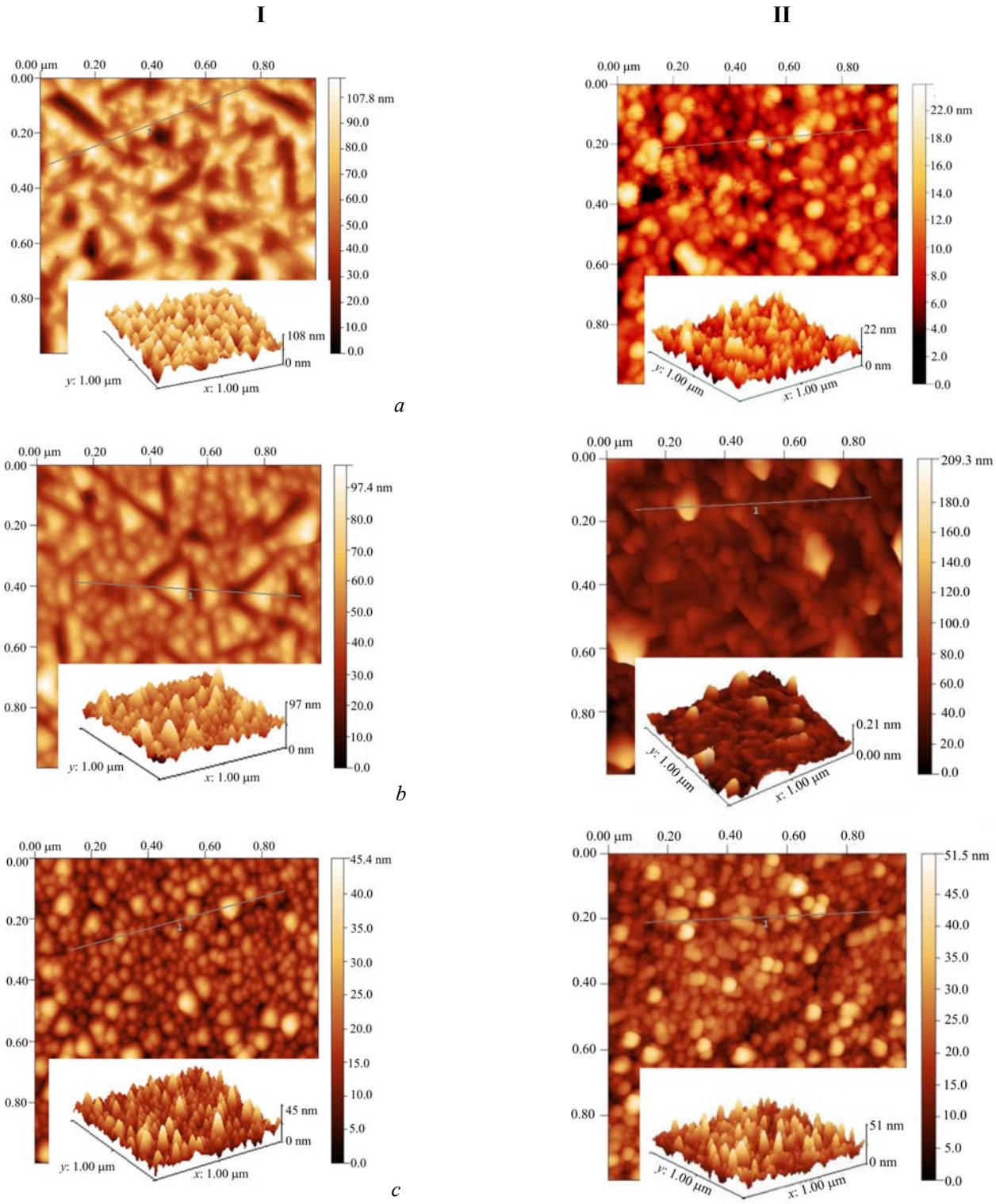

Fig. 1. *2D and 3D AFM-images of PbTe:Bi surface condensates deposited on (0001) cleavages of muscovite mica (I) and sitall (II) substrates in different technological modes:*
a: T_S = 420 K, T_E = 970 K, τ = 900 sec (I), τ = 60 sec (II);
b: T_S = 470 K, T_E = 970 K, τ = 900 sec (I), τ = 60 sec (II);
c: T_S = 470 K, T_E = 970 K, τ = 300 sec (I), τ = 15 sec (II).

Table 1

Technological modes for the PbTe:Bi thin films deposited on (0001) fresh cleavages of muscovite mica and sitall substrates and their morphological characteristics

Sample №	Substrate material	Evaporator temperature T_E, K	Substrate temperature T_E, K	Deposition time τ, sec	Thickness d, nm	Average height h_{av}, m	Average roughness R, nm
2m	mica	970	470	300	320	16	1.8
4m	mica	970	470	900	670	47	2.2
7m	mica	970	420	900	1080	35	1.2
4c	sitall	970	420	15	108	14	1.3
5c	sitall	970	420	60	540	9	0.6
14c	sitall	970	470	60	890	53	3.2

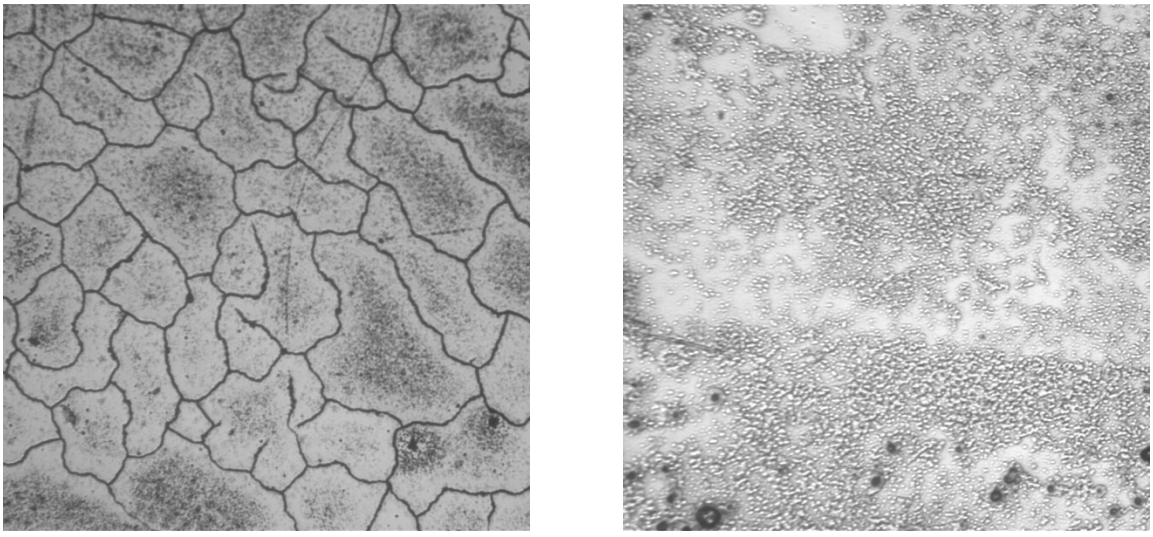

a) *b)*

Fig. 2. The image of the surface of the PbTe:Bi films deposited on mica (a, sample 4m, Table 1) and sitall (b, sample 14c, Table 1) substrates. Surface image obtained at 400x magnification with Nexus 412 A optical microscope (INNOVATEST).

Theory

To optimize the parameters of thermoelectric material, it is necessary to correctly describe the dynamics of the electron and phonon subsystems of the material. As regards the bulk materials, these issues are well described, for example, in surveys [28 – 32]. Often, with sufficiently high accuracy, we can restrict ourselves to taking into account the scattering of charge carriers by acoustic phonons. Sometimes, the interaction of charge carriers with optical phonons or vacancies can play a certain role, especially when the inelastic effects of electron-phonon interaction are significant or a strongly degenerate material is considered.

If thin films are under study, then additional mechanisms should be considered that determine the total contribution of charge carriers scattering. In particular, this is the influence of the surface and grain boundaries.

The consideration of the surface scattering, as well as size-related effects, can have a significant effect on the finite material properties [33]. The first explanations of these effects were given by Fuchs and

Sondheimer [34, 35] by the example of metallic films. As shown in these papers, the influence of the surface and interfaces is determined by the corresponding inelastic scattering of the carriers. The mean free path of the carriers is statistically uniformly distributed over the bulk of material. Therefore, it is considered that the surface itself plays a dominant role in such distribution of the values of the mean free path values. According to this model, the resistivity is determined by next ratio:

$$\frac{\rho_0}{\rho_{FS}} = \frac{k}{\Phi_p(k)} \tag{2}$$

where

$$\frac{k}{\Phi_p(k)} = \frac{1}{k}\frac{3}{2k^2}(1-p)\int_1^{\infty}\left(\frac{1}{t^3}-\frac{1}{t^5}\right)\frac{1-e^{-kt}}{1-pe^{-kt}}dt \tag{3}$$

Here, $\rho_{FS}$is the resistivity due to the influence of the film surface, p_0 is the value of resistance for the bulk material, $k = t/\lambda_0$ is the ratio where λ_0 is mean free path in the bulk material, p – the proportion of elastically scattered electrons by the film surface. If $p = 0$, we obtain the maximum value for p, which completely corresponds to the surface scattering. Assuming that $p = 1$ we have mirror surfaces, which indicates the dominance of volume scattering and neglecting the surface influence.

Analytically, the contribution of these mechanisms to total mobility can be expressed by following ratio:

$$\frac{\mu}{\mu_{bulk}} = 1 - \frac{3\lambda}{8D}(1-p), \tag{4}$$

where λ is mean free path, D is film thickness, p is surface reflection coefficient .

Mayadas and M. Shatzkes developed the Fuchs and Sondheimer theory for the case of taking into account carrier scattering on grain boundaries [36]. The main parameter in this case was the grain size D:

$$\frac{\rho_0}{\rho_{MS}} = \left[1 - \frac{2}{3}\alpha + 3\alpha^2 - 3\alpha^3 \ln\left(1+\frac{1}{\alpha}\right)\right]^{-1} \tag{5}$$

where $\alpha = \frac{\lambda}{D}\left(\frac{R}{1-R}\right)$, R is grain boundary reflection coefficient which takes on the values from 0 to 1.

Then, taking into account the influence of grain boundaries on the charge carrier mobility is determined by ratio [36]:

$$\frac{\mu}{\mu_{bulk}} = \frac{1}{1+1.34\left(\frac{R}{R-1}\right)\frac{\lambda}{d_{grain}}}, \tag{6}$$

where d_{grain} is the average grain size.

In [37], a certain combined model was proposed for thin films. The values of the p and R coefficients were taken in this case from the experimental results. Accordingly, the total resistance was determined:

$$\rho_{sum} = \rho_{FS} + \rho_{MS} - \rho_0 . \tag{7}$$

The appropriate combinations of values p and R were selected [38] for the best agreement with the experimental data.

Results and discussion

The analysis of the AFM images was performed for reasons of determining the influence of surface temperature, deposition time, and substrate material on the surface of the resulting condensates. In this way one can get information on the mechanisms of the nucleation and growth of the obtained thin films. The theoretical basis for explaining these processes is rather fully formulated in [39, 40].

As can be seen from Fig.1, irrespective of the deposition conditions and substrate material, the PbTe:Bi thin films tend to formation and growth of individual pyramidal structures. The formation of three-dimensional individual initial islands indicates the implementation of the Folmer-Weber growth mechanism. However, there are some differences, depending on the choice of substrate material. Thus, it is clearly seen that pyramidal nanoislands of correct cut with a triangular basis grow on mica crystalline substrates. No formation of the objects of clear symmetry group is observed on polycrystalline sitall substrates. However, in both cases, it can be argued that there is certain degree of uniformity in the distribution of nanoobjects along the film surface, for which, both normal and lateral dimensions exceed the mean free path of charge carriers and make up (50 – 200) nanometers.

The analysis of the deposition time shows a certain pattern. The time of deposition is the most significant factor that forms the geometry of nanostructures surface. The change in the substrate temperature slightly changes their average height, while the change in the deposition time (in particular, decrease) causes the formation of several fold smaller nanoislands in the lateral direction. As regards the substitution of substrate for sitall, it can be seen that the dimensions of pyramidal structures are affected by the change in the deposition time and the change in the substrate temperature. Still, the choice of substrate temperature is more decisive in their geometry. Thus, a slight change in temperature can cause an increase in the size of nanoislands by almost 10 times. Therefore, in the case of sitall, one can definitely assert the implementation of the Folmer-Weber mechanism of nucleation. As for monocrystalline mica substrates, the growth rate is slightly slower, although the deposition time was much longer. But on the basis of the fact that monocrystalline substrates are more structurally perfect, one can assume that in this case the implementation of the nucleation mechanism of the Stranky-Krastanov can be more obvious. When this occurs, the layer growth is first realized, and then three-dimensional islands are formed on the surface.

On the other hand, the logarithmic normal distribution is observed along the heights of surface nanostructures for both substrate materials, which is confirmed by the AFM data and described in [41]. This indicates the perfection of the deposited material within the grain. Therefore, when considering thermoelectric parameters, the effects that are realized in the bulk materials and the specific effects associated with the surface are more significant.

As shown in [42], the transition from the bulk materials to films substantially reduces the value of the coefficient of thermal conductivity. According to (1), this leads to significant increase of the thermoelectric Q-factor.

The scattering mechanisms for the bulk materials that determine thermoelectric parameters are studied in detail, for example, in [31]. Therefore, in this publication an estimation of the effects associated with the contribution of surface to total scattering of charge carriers was made. In particular, the influence of the surface according to with expression (4) and the influence of grain boundaries according to expression (6) were estimated. The analysis was performed for thin films deposited on different substrates, since different structure of substrates can contribute to the implementation of various scattering mechanisms.

As for the calculated values, it is necessary to pay special attention to the values of the mean free path of carriers. Different papers presented different meanings, which were, however, approximately of the same order. In particular, a λ value of 40 nm [43], 10 nm [44], or an interval from 10 nm to 100 nm [45] were obtained. The first two values are calculated, derived from the *ab initio* methods. Our calculations,

according to method [46] showed a value of 72 nm, which is in good agreement with the results of the above studies.

The grain size was determined using a Nexus 412 A (INNOVATEST) optical microscope.

The technological modes and characteristics of deposited films are presented in Tables 2-3.

Table 2

Technological parameters of the deposited PbTe:Bi thin films obtained on muscovite mica (samples 2m, 4m, 7m) and sitall (samples 4c, 5c, 14c) substrates.

No samples	Substrate	Evaporator temperature T_E, K	Substrate temperature T_S, K	Deposition time τ, sec	Thickness d, nm	Grain size, μ*m*	Average height value of nanostructures h_c, nm	Average roughness R, nm
2m	mica	970	470	300	320	60	16	1.8
4m	mica	970	470	900	670	80	47	2.2
7m	mica	970	420	900	1080	65	35	1.2
4c	sitall	970	420	15	108	0.4	14	1.3
5c	sitall	970	420	60	540	0.8	9	0.6
14c	sitall	970	470	60	890	3	53	3.2

Table 3

Experimental values of specific conductivity σ, the Hall coefficient R_H, carrier concentration n (p), and charge carrier mobility μ of PbTe:Bi thin films obtained on muscovite mica (samples 2m, 4m, 7m) and sitall (samples 4c, 5c, 14c) substrates.

Sample №	σ, $\Omega^{-1}cm^{-1}$	R_H, cm^3/C	n (p), cm^{-3}	μ, $cm^2/V\ s$
2m	627	-0.039	$-1.6\cdot10^{20}$	24.2
4m	480	-0.030	$-2.1\cdot10^{20}$	14.4
7m	44.0	-0.101	$-6.2\cdot10^{20}$	4.4
4c	6.60	3.49	$8.3\cdot10^{19}$	23
5c	74.5	0.27	$8.3\cdot10^{19}$	20
14c	384	0.13	$8.3\cdot10^{19}$	51

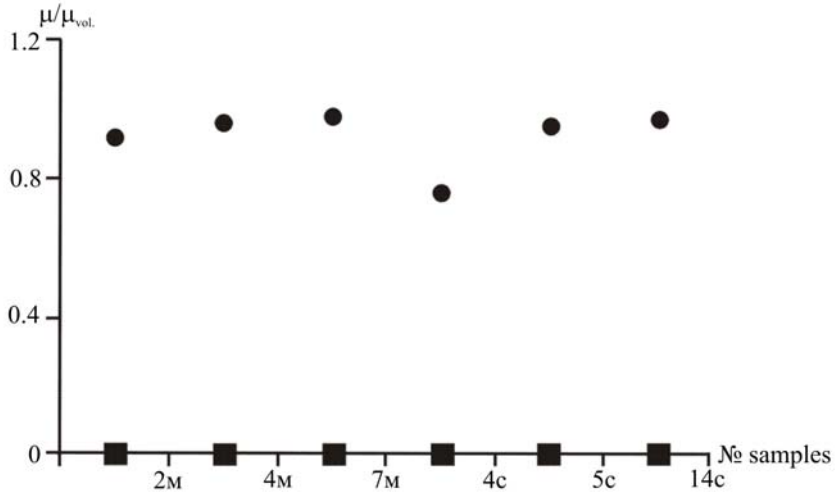

Fig. 3. The relation of $\frac{\mu}{\mu_{bulk}}$*, obtained by taking into account the influence of the surface (circles) and intergrain boundaries (squares).*

The estimate of the effect of charge carrier scattering on the surface and at the intergrain boundaries is shown in Fig. 3. The proximity of the ratio μ/μ_{bulk} to unity indicates that the total mobility obtained by the Mattisen rule is determined mainly by the scattering mechanisms inherent in the bulk materials (carrier scattering on phonons or vacancies). The greater the deviation from the unity, the greater the influence of surface effects. As can be seen in Fig. 3, account of the surface mobility μ_{FS} (the Fuchsian and Zondheim theory) is significant for the sample 4c. This is well explained if we analyze the thickness of all studied films. It is for this sample that the thickness is the smallest and is 108 nm (Table 2).

If we consider the influence of intergrain boundaries, this effect will be dominant for all films (curve 2 – Fig. 3) and determined by mobility μ_{MS} (the Mayadas and Shatzkes theory).

The effect of film thickness D is in good agreement with the experimental data and the use of a combined model ($\mu_{MS} + \mu_{FS}$) for quantitative estimation of the contributions of surface and grain boundaries to the values of mobility and electrical conductivity. The good agreement between the calculated and the experimental data occurs, provided that the reflection coefficients p and R vary with thickness. This can happen when the main contribution to the measured values causes the grain boundaries to be taken into account. That is, it can be assumed that with increasing film thickness, in the first stages the key role is played by the nucleation processes of the film, which are responsible for the formation of grain boundaries and lead to high values of electrical conductivity (samples *PbTe:Bi* deposited on mica 2m, 4m, Table 2). These results are in good agreement with the data [38], where the authors analyze correlations between the thickness and size of surface formations with the time of growth.

Conclusion

The role of the effects associated with the surface in the analysis of charge carrier scattering mechanisms and, consequently, their influence on the thermoelectric properties of thin films are determined. The dominant influence of carrier scattering on intergrain boundaries (the Mayadas and Shatzkes theory) is established, regardless of the grain size. The influence of the surface effects, which is described by the Fuchs and Sondheimer theory, becomes significant with decreasing the thickness of films. In particular, for *PbTe:Bi*, the surface of the film substantially affects transport phenomena for thicknesses ~ 100 nm, that is, for thin films whose thickness is commensurate with the mean free path. The obtained

results allow setting the technological regimes for optimization of the material parameters in order to obtain the maximum values of thermoelectric figure of merit *ZT*.

References

1. Anatychuk L. I. (2007). Current status and some prospects of thermoelectricity. *J. Thermoelectricity*, 2, 7.
2. Rowe D. M. (2005). *Thermoelectrics handbook: macro to nano*. CRC press.
3. Bell L. E. (2008). Cooling, heating, generating power, and recovering waste heat with thermoelectric systems. *Science*, 321(5895), 1457-1461.
4. Mamur H., Ahiska R. (2014). A review: Thermoelectric generators in renewable energy. *International Journal of Renewable Energy Research (IJRER)*, 4(1), 128-136.
5. Anatychuk L. I., Rozver Y. Y., Misawa K., & Suzuki N. (1997). Thermal generators for waste heat utilization. *Proceedings of XVI International Conference on Thermoelectrics (Dresden, Germany, August 1997) (pp. 586-587).*
6. LeBlanc S., Yee S. K., Scullin M. L., Dames C., & Goodson K. E. (2014). Material and manufacturing cost considerations for thermoelectrics. *Renewable and Sustainable Energy Reviews*, 32, 313-327.
7. Snyder G. J. and Toberer E. S. (2008). Complex thermoelectric materials. *Nature Materials* 7, 105-114.
8. Zhang Q., Liao B., Lan Y., Lukas K., Liu W., Esfarjani K., ... & Ren Z. (2013). High thermoelectric performance by resonant dopant indium in nanostructured SnTe. *Proceedings of the National Academy of Sciences*, 110(33), 13261-13266.
9. Ren Z., Zhang Q., & Chen G. U.S. Patent No. 9,905,744. Washington, DC: U.S. Patent and Trademark Office, 2018.
10. Pei Y. Z., Shi X. Y., LaLonde A., Wang H., Chen L. D. and Snyder G. J. (2011). Convergence of electronic bands for high performance bulk thermoelectrics. *Nature*, 473, 66-69.
11. Mao J., Shuai J., Song S., Wu Y., Dally R., Zhou J., ... & Wilson S. (2017). Manipulation of ionized impurity scattering for achieving high thermoelectric performance in n-type Mg_3Sb_2-based materials. *Proceedings of the National Academy of Sciences*, 2017, 201711725.
12. Horichok I., Ahiska R., Freik D., Nykyruy L., Mudry S., Matkivskiy O., & Semko T. (2016). Phase content and thermoelectric properties of optimized thermoelectric structures based on the Ag-Pb-Sb-Te system. *J.Electronic Materials*, 45(3), 1576-1583.
13. Haluschak M.O., Mudryi S.I., Lopyanko M.A., et al. (2016). Phase composition and thermoelectric properties of materials in Pb-Ag-Te system. *J. Thermoelectricity*, 3, 34-39.
14. Shostakovski P. (2016). The manufactured thermoelectric generators. *Modern Electronics*, 1, 2-5.
15. Dashevsky Z., Kreizman R., & Dariel M. P. (2005). Physical properties and inversion of conductivity type in nanocrystalline PbTe films. *J. Applied Physics*, 98(9), 094309.
16. Freik D.M., Chobanyuk V.M., Nykyruy L.I. (2006). Semiconductors thin films – modern state (the review). *Physics and Chemistry of Solid State*, 7(3), 405-417.
17. Bulman G., Barletta P., Lewis J., Baldasaro N., Manno M., Bar-Cohen A., & Yang B. (2016). Superlattice-based thin-film thermoelectric modules with high cooling fluxes. *Nature Communications*, 7, 10302.
18. Baumgart H., Chen X., Lin P., & Zhang K. (2017). Review of recent progress in nanoscaled thermoelectric thin films. *The Electrochemical Society Meeting Abstracts* (2017, September) (No. 27, pp. 1166-1166).

19. Böttner H., Chen G., & Venkatasubramanian R. (2006). Aspects of thin-film superlattice thermoelectric materials, devices, and applications. *MRS Bulletin*, 31(3), 211-217.
20. Hicks L. D., & Dresselhaus M. S. (1993). Effect of quantum-well structures on the thermoelectric figure of merit. *Physical Review B*, 47(19), 12727.
21. Lan Y., Minnich A. J., Chen G., & Ren Z. (2010). Enhancement of thermoelectric figure of merit by a bulk nanostructuring approach. *Advanced Functional Materials*, 20(3), 357-376.
22. Anatychuk L. I. & Luste O. J. (1996). Physical principles of microminiaturization in thermoelectricity. *Proc Fifteenth International Conference on Thermoelectrics* (Pasadena, USA, 1996, March) (pp. 279-287).
23. Alam H., & Ramakrishna S. (2013). A review on the enhancement of figure of merit from bulk to nano-thermoelectric materials. *Nano Energy*, 2(2), 190-212.
24. Ding D., Wang D., Zhao M., Lv J., Jiang H., Lu C., & Tang Z. (2017). Interface engineering in solution of processed nanocrystal thin films for improved thermoelectric performance. *Advanced Materials*, 29(1), 1603444.
25. Venkatasubramanian R., Silvola E., Colpitts T., & O'quinn B. (2011). Thin-film thermoelectric devices with high room-temperature figures of merit. In *Materials for Sustainable Energy: A Collection of Peer-Reviewed Research and Review Articles from Nature Publishing Group (pp. 120-125) (2011); Moorthy, S. B. K. (Ed.). Thin film structures in energy applications. Springer, 2015.*
26. Moskalyk I. A. (2015). About the use of thermoelectric devices in cryosurgery. *Physics and Chemistry of Solid State*, 16(4), 742-746.
27. Bulman G., Barletta P., Lewis J., Baldasaro N., Manno M., Bar-Cohen A., & Yang B. (2016). Superlattice-based thin-film thermoelectric modules with high cooling fluxes. *Nature Communications*, 7, 10302.
28. Zayachuk D.M. (1997). On the question of the dominant scattering mechanisms in lead telluride. *Semiconductors*, 31, 217–220.
29. Bilc D. I., Mahanti S. D., and Kanatzidis M. G. (2006). Electronic transport properties of PbTe and AgPb m SbTe 2+ m systems. *Physical Review B 74*, 12, 125202.
30. Ahmad Salameh, and Mahanti S. D. (2010). Energy and temperature dependence of relaxation time and Wiedemann-Franz law on PbTe. *Physical Review B* 81, 16, 165203.
31. Freik D.M., Nykyruy L.I., Ruvinskiy M.A., Shperun V.M. and Nyzhnykevych V.V. (2001). Scattering of current carriers in n-type lead chalcogenides crystals. *Physics and Chemistry of Solid State*, 2(4), 681-685.
32. Lee HoSung. (2016). A theoretical model of thermoelectric transport properties for electrons and phonons. *J. Electronic Materials* 45, 2, 1115-1141.
33. Panchenko O.A., Sologub S.V. (2003). Dimensional phenomena and surface scattering of current carriers in metals (review). *Physics and Chemistry of Solid State,* 4(1), 7-42.
34. Fuchs K. (1938). The conductivity of thin metallic films according to the electron theory of metals. *Proc. Camb. Phil. Soc*., 34, 100.
35. Sondheimer E. H. (1952). The mean free path of electrons in metals. *Adv. Phys*. 1, 1.
36. Mayadas A. F. and Shatzkes M. (1970). Electrical resistivity model for polycrystalline films: the case of arbitrary reflection at external surfaces. *Phys. Rev. B*, 1, 1382.
37. Durkan C., Welland M.E. (2000). Size effects in the electrical resistivity of polycrystalline nanowires. *Phys. Rev. B*, 61, 14215.
38. Camacho J.M., Oliva A.I. (2006). Surface and grain boundary contributions in the electrical resistivity of metallic nanofilms. *Thin Solid Films* 515(4), 1881-1885.

39. Vengrenovych R.D., Ivanskyy B.V., Moskalyuk A.V. (2009). The theory of Lifshitz-Slyozov-Wagner. *Physics and Chemistry of Solid State*, 10(1), 19-23.
40. Ivanskii B. V., Vengrenovich R. D., Kryvetskyi V. I., & Kushnir Y. M. (2017). Ostwald ripening of the InAsSbP/InAs (100) quantum dots in the framework of the modified LSW theory. *J. Nano-and Electronic Physics*, 9(2), 2025-1.
41. Saliy Y., Ruvinskiy M. and Nykyruy L. (2017). Statistics of nano-objects characteristics on the surface of PbTe: Bi condensate deposited on ceramic. *Modern Physics Letters B*, 31(03), 1750023.
42. Nykyruy L.I., Ruvinskiy M.A., Ivakin E.V., Kostyuk O.B., Horichok I.V., Kisialiou I.G., Yavorskyy Y.S., Hrubyak A.B. (2018). Low-dimensional systems on the base of PbSnAgTe compounds for thermoelectric application. *Physica E: Low-dimensional systems and nanostructures* (in print); doi: 10.1016/j.physe.2018.10.020.
43. Song Q., Liu T.H., Zhou J., Ding Z. and Chen G. (2017). Ab initio study of electron mean free paths and thermoelectric properties of lead telluride. *Materials Today Physics*, 2, 69-77.
44. Peng-Xian L. and Ling-Bo Q. (2013). Electronic structure, lattice dynamics and thermoelectric properties of PbTe from first-principles calculation. *Chinese Physics Letters*, 30(1), 017101.
45. Liu T.H., Zhou J., Li M., Ding Z., Song Q., Liao B., Fu L. and Chen G. (2018). Electron mean-free-path filtering in Dirac material for improved thermoelectric performance. *Proceedings of the National Academy of Sciences*, 201715477.
46. Ruvinskii M.A., Kostyuk O.B. and Dzundza B.S. (2015). Classic size effects in n-PbTe films. *Physics and Chemistry of Solid State*, 16(4), 661-666.

Submitted 12.06.2018

Никируй Л.І. *канд. фіз.-мат. наук* , *професор*[1],
Возняк О.М. *канд. фіз.-мат. наук* [1],
Яворський Я.С. *канд. фіз.-мат. наук* [1],
Шендеровський В.А. *доктор фіз.-мат. наук,професор* [2],
Дзумедзей Р.О.[1], **Костюк О.Б.**[1],
Запухляк Р.І. *канд. фіз.-мат. наук* , *доцент*[1]

[1]Прикарпатський національний університет імені Василя Стефаника,
вул. Шевченка, 57, м. Івано-Франківськ, 76018, Україна,
[2]Інститут фізики НАН України, пр. Науки, 46, м. Київ, 02000, Україна

ВПЛИВ ПОВЕДІНКИ НОСІЇВ ЗАРЯДУ НА ТЕРМОЕЛЕКТРИЧНІ ВЛАСТИВОСТІ ТОНКИХ ПЛІВОК *PbTe:Bi*

Досліджено вплив технологічних факторів осадження тонких плівок методом відкритого випаровування у вакуумі на реалізацію процесів розсіювання носіїв заряду. Для плівок PbTe:Bi, осаджених на підкладки (0001) слюди-мусковіт та ситалу визначено внесок у транспортні явища механізмів розсіювання носіїв, пов'язаних із поверхнею (теорія Фукса і Зондгеймера) та із межами зерен (теорія Мейядеса та Шацкиса). Вибором типу матеріалу підкладки та температурних режимів осадження змінювали структуру поверхні плівки та, відповідно, термоелектричні параметри вихідного матеріалу. Зокрема, підбір експериментальних режимів дозволяє маніпулювати розмірами зерен та товщиною плівки. Скло-керамічні підкладки із

ситалу сприяють отриманню суттєво менших розмірів зерен у порівнянні із використанням підкладок із слюди. Показано, що ефекти, пов'язані із розсіюванням на межах зерен є домінуючими для всіх плівок. Поверхневі ж ефекти стають суттєвими лише для достатньо тонких плівок, для яких товщина співмірна із довжиною вільного пробігу носії заряду. Бібл.46, рис.3, табл.2.

Ключові слова: термоелектрика, тонкі плівки, поверхня, межі зерен, механізми розсіювання носіїв.

Никируй Л.И. *канд. физ.-мат. наук* , *професор*[1]**,**
Возняк О.М. *канд. физ.-мат. наук* [1]**,**
Яворский Я.С. *канд. физ.-мат. наук* [1]**,**
Шендеровский В.А. *доктор физ.-мат. наук,професор* [2]**,**
Дзумедзей Р.О.[1]**, Костюк О.Б.**[1]**,**
Запухляк Р.И. *канд. физ.-мат. наук* , *доцент*[1]

[1]Прикарпатский национальный университет имени Василия Стефаныка,
ул. Шевченка, 57, г. Ивано-Франковск, 76018, Украина,
[2]Институт физики НАН Украины, пр. Науки, 46,
г. Киев, 02000, Украина

ВЛИЯНИЕ ПОВЕДЕНИЯ НОСИТЕЛЕЙ ЗАРЯДА НА ТЕРМОЭЛЕКТРИЧЕСКИЕ СВОЙСТВА ТОНКИХ ПЛЕНОК *PbTe*:*Bi*

Исследовано влияние технологических факторов осаждения тонких пленок методом открытого испарения в вакууме на реализацию процессов рассеяния носителей заряда. Для пленок PbTe:Bi, осажденных на подложки (0001) слюды-мусковит и ситалла определен взнос в транспортные явления механизмов рассеяния носителей, связанных с поверхностью (теория Фукса и Зондгеймера) и с границами зерен (теория Мейядеса и Шацкиса). Выбором типа материала подложки и температурных режимов осаждения изменяли структуру поверхности пленки и, соответственно, значения термоэлектрических параметров исходного материала. В частности, подбор экспериментальных режимов позволяет манипулировать размерами зерен и толщиной пленки. Стеклокерамические подложки из ситалла способствуют получению существенно меньших размеров зерен исходных пленок в сравнении с использованием подложек из слюды. Показано, что эффекты, связанные с рассеянием на границах зерен, являются доминирующими для всех пленок. Поверхностные же эффекты становятся существенными только для достаточно тонких пленок, толщина которых соразмерна с длиной свободного пробега носителей заряда. Библ.46, рис.3, табл.2.

Ключевыеслова: термоэлектричество, тонкиепленки, поверхность, границы зерен, рассеяние носителей заряда.

References

1. Anatychuk L. I. (2007). Current status and some prospects of thermoelectricity. *J. Thermoelectricity*, 2, 7.
2. Rowe D. M. (2005). *Thermoelectrics handbook: macro to nano*. CRC press.
3. Bell L. E. (2008). Cooling, heating, generating power, and recovering waste heat with thermoelectric systems. *Science*, 321(5895), 1457-1461.

4. Mamur H., Ahiska R. (2014). A review: Thermoelectric generators in renewable energy. *International Journal of Renewable Energy Research (IJRER)*, 4(1), 128-136.
5. Anatychuk L. I., Rozver Y. Y., Misawa K., & Suzuki N. (1997). Thermal generators for waste heat utilization. *Proceedings of XVI International Conference on Thermoelectrics (Dresden, Germany, August 1997) (pp. 586-587)*.
6. LeBlanc S., Yee S. K., Scullin M. L., Dames C., & Goodson K. E. (2014). Material and manufacturing cost considerations for thermoelectrics. *Renewable and Sustainable Energy Reviews*, 32, 313-327.
7. Snyder G. J. and Toberer E. S. (2008). Complex thermoelectric materials. *Nature Materials* 7, 105-114.
8. Zhang Q., Liao B., Lan Y., Lukas K., Liu W., Esfarjani K., ... & Ren Z. (2013). High thermoelectric performance by resonant dopant indium in nanostructured SnTe. *Proceedings of the National Academy of Sciences*, 110(33), 13261-13266.
9. Ren Z., Zhang Q., & Chen G. U.S. Patent No. 9,905,744. Washington, DC: U.S. Patent and Trademark Office, 2018.
10. Pei Y. Z., Shi X. Y., LaLonde A., Wang H., Chen L. D. and Snyder G. J. (2011). Convergence of electronic bands for high performance bulk thermoelectrics. *Nature*, 473, 66-69.
11. Mao J., Shuai J., Song S., Wu Y., Dally R., Zhou J., ... & Wilson S. (2017). Manipulation of ionized impurity scattering for achieving high thermoelectric performance in n-type Mg_3Sb_2-based materials. *Proceedings of the National Academy of Sciences*, 2017, 201711725.
12. Horichok I., Ahiska R., Freik D., Nykyruy L., Mudry S., Matkivskiy O., & Semko T. (2016). Phase content and thermoelectric properties of optimized thermoelectric structures based on the Ag-Pb-Sb-Te system. *J.Electronic Materials*, 45(3), 1576-1583.
13. Haluschak M.O., Mudryi S.I., Lopyanko M.A., et al. (2016). Phase composition and thermoelectric properties of materials in Pb-Ag-Te system. *J. Thermoelectricity*, 3, 34-39.
14. Shostakovski P. (2016). The manufactured thermoelectric generators. *Modern Electronics*, 1, 2-5.
15. Dashevsky Z., Kreizman R., & Dariel M. P. (2005). Physical properties and inversion of conductivity type in nanocrystalline PbTe films. *J. Applied Physics*, 98(9), 094309.
16. Freik D.M., Chobanyuk V.M., Nykyruy L.I. (2006). Semiconductors thin films – modern state (the review). *Physics and Chemistry of Solid State*, 7(3), 405-417.
17. Bulman G., Barletta P., Lewis J., Baldasaro N., Manno M., Bar-Cohen A., & Yang B. (2016). Superlattice-based thin-film thermoelectric modules with high cooling fluxes. *Nature Communications*, 7, 10302.
18. Baumgart H., Chen X., Lin P., & Zhang K. (2017). Review of recent progress in nanoscaled thermoelectric thin films. *The Electrochemical Society Meeting Abstracts* (2017, September) (No. 27, pp. 1166-1166).
19. Böttner H., Chen G., & Venkatasubramanian R. (2006). Aspects of thin-film superlattice thermoelectric materials, devices, and applications. *MRS Bulletin*, 31(3), 211-217.
20. Hicks L. D., & Dresselhaus M. S. (1993). Effect of quantum-well structures on the thermoelectric figure of merit. *Physical Review B*, 47(19), 12727.
21. Lan Y., Minnich A. J., Chen G., & Ren Z. (2010). Enhancement of thermoelectric figure of merit by a bulk nanostructuring approach. *Advanced Functional Materials*, 20(3), 357-376.
22. Anatychuk L. I. & Luste O. J. (1996). Physical principles of microminiaturization in thermoelectricity. *Proc Fifteenth International Conference on Thermoelectrics* (Pasadena, USA, 1996, March) (pp. 279-287).

23. Alam H., & Ramakrishna S. (2013). A review on the enhancement of figure of merit from bulk to nano-thermoelectric materials. *Nano Energy*, 2(2), 190-212.
24. Ding D., Wang D., Zhao M., Lv J., Jiang H., Lu C., & Tang Z. (2017). Interface engineering in solution of processed nanocrystal thin films for improved thermoelectric performance. *Advanced Materials*, 29(1), 1603444.
25. Venkatasubramanian R., Silvola E., Colpitts T., & O'quinn B. (2011). Thin-film thermoelectric devices with high room-temperature figures of merit. In *Materials for Sustainable Energy: A Collection of Peer-Reviewed Research and Review Articles from Nature Publishing Group (pp. 120-125) (2011); Moorthy, S. B. K. (Ed.). Thin film structures in energy applications. Springer, 2015.*
26. Moskalyk I. A. (2015). About the use of thermoelectric devices in cryosurgery. *Physics and Chemistry of Solid State*, 16(4), 742-746.
27. Bulman G., Barletta P., Lewis J., Baldasaro N., Manno M., Bar-Cohen A., & Yang B. (2016). Superlattice-based thin-film thermoelectric modules with high cooling fluxes. *Nature Communications*, 7, 10302.
28. Zayachuk D.M. (1997). On the question of the dominant scattering mechanisms in lead telluride. *Semiconductors*, 31, 217–220.
29. Bilc D. I., Mahanti S. D., and Kanatzidis M. G. (2006). Electronic transport properties of PbTe and AgPb m SbTe 2+ m systems. *Physical Review B 74*, 12, 125202.
30. Ahmad Salameh, and Mahanti S. D. (2010). Energy and temperature dependence of relaxation time and Wiedemann-Franz law on PbTe. *Physical Review B* 81, 16, 165203.
31. Freik D.M., Nykyruy L.I., Ruvinskiy M.A., Shperun V.M. and Nyzhnykevych V.V. (2001). Scattering of current carriers in n-type lead chalcogenides crystals. *Physics and Chemistry of Solid State*, 2(4), 681-685.
32. Lee HoSung. (2016). A theoretical model of thermoelectric transport properties for electrons and phonons. *J. Electronic Materials* 45, 2, 1115-1141.
33. Panchenko O.A., Sologub S.V. (2003). Dimensional phenomena and surface scattering of current carriers in metals (review). *Physics and Chemistry of Solid State,* 4(1), 7-42.
34. Fuchs K. (1938). The conductivity of thin metallic films according to the electron theory of metals. *Proc. Camb. Phil. Soc*., 34, 100.
35. Sondheimer E. H. (1952). The mean free path of electrons in metals. *Adv. Phys*. 1, 1.
36. Mayadas A. F. and Shatzkes M. (1970). Electrical resistivity model for polycrystalline films: the case of arbitrary reflection at external surfaces. *Phys. Rev. B*, 1, 1382.
37. Durkan C., Welland M.E. (2000). Size effects in the electrical resistivity of polycrystalline nanowires. *Phys. Rev. B*, 61, 14215.
38. Camacho J.M., Oliva A.I. (2006). Surface and grain boundary contributions in the electrical resistivity of metallic nanofilms. *Thin Solid Films* 515(4), 1881-1885.
39. Vengrenovych R.D., Ivanskyy B.V., Moskalyuk A.V. (2009). The theory of Lifshitz-Slyozov-Wagner. *Physics and Chemistry of Solid State*, 10(1), 19-23.
40. Ivanskii B. V., Vengrenovich R. D., Kryvetskyi V. I., & Kushnir Y. M. (2017). Ostwald ripening of the InAsSbP/InAs (100) quantum dots in the framework of the modified LSW theory. *J. Nano-and Electronic Physics*, 9(2), 2025-1.
41. Saliy Y., Ruvinskiy M. and Nykyruy L. (2017). Statistics of nano-objects characteristics on the surface of PbTe: Bi condensate deposited on ceramic. *Modern Physics Letters B*, 31(03), 1750023.
42. Nykyruy L.I., Ruvinskiy M.A., Ivakin E.V., Kostyuk O.B., Horichok I.V., Kisialiou I.G., Yavorskyy Y.S., Hrubyak A.B. (2018). Low-dimensional systems on the base of PbSnAgTe compounds for

thermoelectric application. *Physica E: Low-dimensional systems and nanostructures* (in print); doi: 10.1016/j.physe.2018.10.020.

43. Song Q., Liu T.H., Zhou J., Ding Z. and Chen G. (2017). Ab initio study of electron mean free paths and thermoelectric properties of lead telluride. *Materials Today Physics*, 2, 69-77.
44. Peng-Xian L. and Ling-Bo Q. (2013). Electronic structure, lattice dynamics and thermoelectric properties of PbTe from first-principles calculation. *Chinese Physics Letters*, 30(1), 017101.
45. Liu T.H., Zhou J., Li M., Ding Z., Song Q., Liao B., Fu L. and Chen G. (2018). Electron mean-free-path filtering in Dirac material for improved thermoelectric performance. *Proceedings of the National Academy of Sciences*, 201715477.
46. Ruvinskii M.A., Kostyuk O.B. and Dzundza B.S. (2015). Classic size effects in n-PbTe films. *Physics and Chemistry of Solid State*, 16(4), 661-666.

Submitted 12.06.2018